Biochimica et Biophysica Acta 1798 (2010) 1062–1072

Contents lists available at ScienceDirect

Biochimica et Biophysica Acta

journal homepage: www.elsevier.com/locate/bbamem

Structure–function studies of chemokine-derived carboxy-terminal antimicrobial peptides

Leonard T. Nguyen [a], David I. Chan [a], Laura Boszhard [b], Sebastian A.J. Zaat [b], Hans J. Vogel [a,*]

[a] Structural Biology Research Group, Department of Biological Sciences, University of Calgary, 2500 University Dr. NW, Calgary, Alberta, Canada T2N 1N4
[b] Department of Medical Microbiology, Centre for Infection and Immunity Amsterdam (CINIMA), Academic Medical Center, Meibergdreef 15, 1105 AZ Amsterdam, The Netherlands

ARTICLE INFO

Article history:
Received 20 August 2009
Received in revised form 23 November 2009
Accepted 30 November 2009
Available online 11 December 2009

Keywords:
Chemokine
antimicrobial peptide
host defence peptide
innate immunity
peptide structure
peptide-membrane interactions
NMR spectroscopy

ABSTRACT

Recent reports which show that several chemokines can act as direct microbicidal agents have drawn renewed attention to these chemotactic signalling proteins. Here we present a structure–function analysis of peptides derived from the human chemokines macrophage inflammatory protein-3α (MIP-3α/CCL20), interleukin-8 (IL-8), neutrophil activating protein-2 (NAP-2) and thrombocidin-1 (TC-1). These peptides encompass the C-terminal α-helices of these chemokines, which have been suggested to be important for the direct antimicrobial activities. Far-UV CD spectroscopy showed that the peptides are unstructured in aqueous solution and that a membrane mimetic solvent is required to induce a helical secondary structure. A co-solvent mixture was used to determine solution structures of the peptides by two-dimensional ^{1}H-NMR spectroscopy. The highly cationic peptide, MIP-3α$_{51-70}$, had the most pronounced antimicrobial activity and displayed an amphipathic structure. A shorter version of this peptide, MIP-3α$_{59-70}$, remained antimicrobial but its structure and mechanism of action were unlike that of the former peptide. The NAP-2 and TC-1 proteins differ in their sequences only by the deletion of two C-terminal residues in TC-1, but intact TC-1 is a very potent antimicrobial while NAP-2 is inactive. The corresponding C-terminal peptides, NAP-2$_{50-70}$ and TC-1$_{50-68}$, had very limited and no bactericidal activity, respectively. This suggests that other regions of TC-1 contribute to its bactericidal activity. Altogether, this work provides a rational structural basis for the biological activities of these peptides and proteins and highlights the importance of experimental characterization of peptide fragments as distinct entities because their activities and structural properties may differ substantially from their parent proteins.

1. Introduction

Antimicrobial peptides and chemokines were originally thought to have distinct roles in the innate immune response. The former are identified through their direct interactions with and killing actions on invading microbes and the latter through their role in inducing leukocyte trafficking. However, these two groups of secreted molecules share many common properties although they have different primary sequences [1–4]. As host-defense molecules of the immune system, the expression levels of defensins and chemokines can be upregulated together in response to microbial challenges [5,6]. Most importantly, there is some overlap in function as some defensins are now known to be capable of activating specific chemokine receptors [2,7,8]. Conversely, many chemokines have recently been shown to exhibit direct antimicrobial activity [9–11]. Like conventional antimicrobial peptides, these chemokines have net positive charges with pI's greater than 9.0. A structural survey indicated that large positively charged patches on the molecular surface are a common theme found in antimicrobial chemokines, but not in nonantimicrobial chemokines [10]. Peptide cationicity favors interactions with negatively charged moieties on the surface of microbial membranes over zwitterionic mammalian membranes [12]. The best documented example of an antimicrobial chemokine is the human macrophage inflammatory protein-3α (MIP-3α), also known as CC chemokine ligand 20 (CCL20) [10,13]. MIP-3α is active at low effective concentrations against a wide range of organisms, including Gram-positive and Gram-negative bacterial species, as well as fungi [10]. Against *Escherichia coli*, the chemokine is more potent than several human β-defensins. Similar to defensins and many other antimicrobial peptides, this activity is salt-sensitive, which suggests that charge interactions play a major role in the activity [14,15]. Of all the chemokines, MIP-3α is functionally linked to the β-defensins through their ability to activate the CC chemokine receptor-6 (CCR6) [16,17], which is otherwise rather specific and does not interact with any other chemokines [18,19].

In tumor progression, the chemotactic activity of MIP-3α can be inactivated by cathepsin D proteolytic processing [20]. This process releases a 12-aa C-terminal peptide fragment of MIP-3α that can act

* Corresponding author. Tel.: +1 403 220 6006; fax: +1 403 289 9311.
E-mail address: vogel@ucalgary.ca (H.J. Vogel).

0005-2736/$ – see front matter © 2009 Elsevier B.V. All rights reserved.
doi:10.1016/j.bbamem.2009.11.021

as an antimicrobial agent. The second major product, encompassing the first 55 residues of the 70-aa MIP-3α protein, is inactive against bacteria. The antimicrobial region is part of the C-terminal α-helix in MIP-3α that begins at Thr54. This α-helix is highly amphipathic with large aliphatic and aromatic sidechains making hydrophobic contacts with residues of the antiparallel β-sheet and positively charged sidechains facing the exterior of the protein [21,22]. A peptide corresponding to the entire α-helix and its flanking residues is unstructured in aqueous solution, but adopts the native secondary structure in membrane mimetic environments [21]. This behavior is characteristic of most members of the α-helical class of antimicrobial peptides such as the magainins and cecropins [23,24] and has also been observed with lactoferrampin, another cationic antimicrobial peptide derived from a large protein [25,26]. Further work shows that some α-helical antimicrobial peptides can adopt helix-break-helix structures [27], helical hairpins upon complexation with LPS [28], or antiparallel dimers or higher oligomeric states to help penetrate membranes [29,30].

Another cationic CXC chemokine, interleukin-8 (IL-8), has mild to nonexistent antimicrobial activity depending on the assay conditions used and the bacterium tested. IL-8 is generally inactive against *E. coli* and *Staphylococcus aureus* but it is inhibitory against *Salmonella typhimurium* [10,31,32]. Interestingly, peptide fragments encompassing the C-terminal α-helix of IL-8 are more potent as antimicrobials compared to the parent protein, most notably against *E. coli* in solid-state and whole blood assays [31,32]. This suggests that the remainder of the IL-8 protein may obstruct the full antimicrobial potential of this segment.

The far C-terminal region is also important in the CXC chemokine neutrophil-activating protein-2 (NAP-2), which is known to bind the same chemokine receptor as IL-8 [33]. NAP-2 is isolated from human platelets and the intact protein displays low antimicrobial activity. A NAP-2 variant with a two-residue C-terminal truncation has been isolated and the resulting product not only exhibits higher neutrophil-stimulating capacity [34], but it is also highly bactericidal and fungicidal [35]. The activity of this product, named thrombocidin-1 (TC-1), again highlights the importance of the C-terminal region of chemokines for microbicidal activity. TC-1 has been found to be an important host defence factor in human platelets against infective endocarditis due to *Viridans streptococci* [36]. Products of more extensive C-terminal truncations of NAP-2 have previously been discovered *in vivo*, although their consequence for antimicrobial activity is unknown at present [34,37]. Isolated products of C-terminal processing of MIP-3α, IL-8 and NAP-2 are shown in Table 1 with available antimicrobial activity data.

In this work, we have used NMR and CD spectroscopy to characterize the structures of peptides corresponding to the C-terminal α-helical regions of MIP-3α, IL-8, NAP-2 and TC-1. Their biological activities were measured; moreover vesicle leakage assays were performed by fluorescence spectroscopy to investigate their mode of action. These structure–function analyses allow us to explore these isolated chemokine fragments as potential future antibiotics and provide insight into their role in the overall microbicidal properties of the parent chemokines.

2. Materials and methods

All the synthetic peptides were obtained at >95% purity from 21st Century Biochemicals (Marlboro, MA). The concentrations of MIP-3α$_{51–70}$ and IL-8$_{53–72}$ were calculated by UV absorption at 280 nm using extinction coefficients determined by ProtParam [38]. The concentrations of the peptides without aromatic sidechains, MIP-3α$_{59–70}$, NAP-2$_{50–70}$ and TC-1$_{50–68}$, were determined by weight. All lipids (chicken egg L-α-phosphatidylcholine, ePC; chicken egg L-α-phosphatidylglycerol, ePG; cholesterol) and the lipid extrusion apparatus were purchased from Avanti Polar Lipids (Alabaster, AL).

Table 1
Naturally isolated C-terminal truncation products of the chemokines MIP-3α, IL-8 and NAP-2 and their antimicrobial activities.

Peptide	Sequence	Antimicrobial activities[a]	Ref.
MIP-3α/ CCL20	ASNFDCCLGY TDKILHPKFI VGRTRQLANE GCDINAIIFH TKKKLSVCAN PKQTWVKYIV RLLSKKVKNM	*E. coli*, *S. aureus*, *P. aeruginosa*, *M. catarrhalis*, *S. pyogenes*, *E. faecium*, *C. albicans*, *C. neoformans*	[10]
CCL20$_{1–66}$	ASNFDCCLGY TDKILHPKFI VGRTRQLANE GCDINAIIFH TKKKLSVCAN PKQTWVKYIV RLLSKK	*E. coli*	[20]
CCL20$_{59–70}$	IVRLLSKKVK NM	*E. coli*	[20]
IL-8	SAKELRCQCI KTYSKPFHPK FIKELRVIES GPHCANTEII VKLSDGRELC LDPKENWVQR VVEKFLKRAE NS	*S. typhimurium*, low activity for *E. coli*, *S. aureus* and *C. albicans*	[10, 31, 32]
hIL-8 C-peptide	CLDPKENWVQ RVVEKFLKRA ENS	-	[85]
NAP-2	AELRCMCIKT TSGIHPKNIQ SLEVIGKGTH CNQVEVIATL KDGRKICLDP DAPRIKKIVQ KKLAGDESAD	No activity	[35]
NAP-2 (1–66)	AELRCMCIKT TSGIHPKNIQ SLEVIGKGTH CNQVEVIATL KDGRKICLDP DAPRIKKIVQ KKLAGD	-	[34]
NAP-2 (1–63)	AELRCMCIKT TSGIHPKNIQ SLEVIGKGTH CNQVEVIATL KDGRKICLDP DAPRIKKIVQ KKL	-	[37]
TC-1	AELRCMCIKT TSGIHPKNIQ SLEVIGKGTH CNQVEVIATL KDGRKICLDP DAPRIKKIVQ KKLAGDES	*B. subtilis*, *E. coli*, *S. aureus*, *L. lactis*, *C. neoformans*	[35]

[a] Peptides for which no antimicrobial data has been reported are indicated by a dash.

2.1. CD spectroscopy

The peptides' secondary structures were estimated by circular dichroism (CD) spectroscopy in the far UV range (185–260 nm). Spectra for each sample were recorded on a J-810 spectropolarimeter (Jasco, Tokyo, Japan) at a scanning rate of 200 nm/min, 1 nm band width, 0.5 nm resolution. Ten scans were accumulated and averaged for each sample. 10 μM peptide was used in each sample using water and different concentrations of TFE in % v/v as solvent, going from 0% to 70% TFE in increments of 10%. Mean residue molar ellipticities, $[\theta]$, in deg cm^2 dmol^{-1} were calculated using the formula: $[\theta] = [\theta]_{obs} / 10ncd$ where $[\theta]_{obs}$ is the experimentally measure ellipticity in millideg, n is the number of residues, c is the molar peptide concentration, and d is the optical pathlength of the cell in cm. All CD spectra were acquired at room temperature and analyzed for α-helical content by curve fitting using the SELCON 3 program [39,40] of the CD Pro software package (http://lamar.colostate.edu/~sreeram/CDPro). Data from 50 proteins, including 13 membrane proteins, was used as the reference set for curve fitting of the spectra.

2.2. NMR spectroscopy and structure calculations

For NMR samples, ~2 mg of peptide was dissolved in 500 μL of 4:4:1 CD_3OH:$CDCl_3$:H_2O, except for MIP-3α$_{59–70}$ which was dissolved in a 100-fold excess of SDS micelles. Two-dimensional NOESY, TOCSY, and DQF-COSY spectra were acquired for each peptide at 25 °C on Bruker Avance 600 and 700 MHz spectrometers (Bio-NMR Center, University of Calgary, Alberta, Canada). The 700 MHz spectrometer is equipped with a triple resonance inverse cryoprobe with single axis z-gradient. 2048×600 complex data points were acquired for the

NOESY and TOCSY experiments, with respective mixing times of 250 ms and 120 ms except for the MIP-3α_{59-70} sample in SDS micelles, which had respective mixing times of 100 ms and 80 ms. The DQF-COSY spectra were acquired with 4096×512 complex data points. The spectral sweep widths were 10 ppm. Solvent suppression was achieved using excitation sculpting [41], and the methanol signal was used as a chemical shift reference. Spectra were processed using NMRPipe [42].

The NMRView 5.0.4 software package [43] was used for spectral analysis. Resonance assignment was achieved by standard methods [44]. The program ARIA 1.2 [45,46] was used for structure calculations. In addition to the meaningful inter- and intra-residue nOe's, broad Φ dihedral angle restraints between −35° and −175° were used for non-Pro and non-Gly residues. Default parameters were used in each ARIA run, however in the last two iterations of the last run the numbers of structures calculated were increased from 20 to 40 and 150. The 20 lowest energy structures of the last iterations were retained and their dihedral angles were analyzed using Procheck 3.2 [47]. Structures were visualized using MOLMOL [48]. Hydrophobic moments (μ_H) of the α-helices were calculated from the Totalizer module of MPEx (http://blanco.biomol.uci.edu/mpex) which uses the experimentally based interfacial Wimley–White hydrophobicity scales [49].

2.3. Bactericidal assays

The peptides were tested for microbicidal activities against *Bacillus subtilis* ATCC6633, *E. coli* ML35, and *S. aureus* 42D as previously described [21,43]. Suspensions of logarithmically growing test bacteria were incubated in a microtiter plate at a concentration of 10^5 colony-forming units/mL with peptides in serial 2-fold dilutions. The total incubation volume was 100 μL, using 10 mM phosphate buffer pH 7.0 supplemented with 1% (v/v) of tryptic soy broth (TSB). At time 0 h and after 2 h of incubation on a rotary shaker (300 rpm) at 37 °C, 10 μL aliquots were collected and plated on blood agar plates and incubated overnight at 37 °C. The concentration of peptide eliminating all growth, killing >99.9% of the inoculum, at 2 h is the 99.9% Lethal Dose ($LD_{99.9}$). These experiments were performed in duplicate.

2.4. Hemolytic assays

Hemolytic activity was tested using fresh human red blood cells. Blood collected in EDTA was added to PBS (10 mM phosphate buffer, 130 mM NaCl, pH 7.4) and centrifuged at 200×g for 15 min. The upper layer of pelleted cells was removed, leaving a pellet enriched in erythrocytes. These cells were washed three times in PBS and 1% suspensions (v/v) were prepared in this buffer. Serial dilutions of peptides were prepared in 0.01% acetic acid in a polypropylene microtiter plate (Costar, Cambridge, USA). To 5 μL of diluted peptide, 45 μL of the erythrocyte suspensions were added. Incubations without peptide and with 1% Triton X-100 served as negative and positive controls, respectively. Mixtures were incubated at 37 °C for 60 min and subsequently centrifuged at 1000×*g* for 5 min. The supernatant was transferred to a new microtiter plate and hemoglobin was measured spectrophotometrically at 540 nm. Hemolysis was expressed as a percentage of hemolysis of the 1% Triton X-100 positive control. Experiments were performed in quadruplicate.

2.5. Calcein leakage

A standard calcein leakage assay [50] was performed using preparations of large unilamellar vesicles (LUVs) composed of 1:1 ePC:ePG and 2.5:1 ePC:cholesterol to represent bacterial and mammalian membranes, respectively [51]. Films were formed in glass vials by evaporation from stock aliquots of the appropriate lipids. The lipid films were suspended by vortexing in leakage buffer (10 mM Tris, 150 mM NaCl, 1 mM EDTA, pH 7.4) containing 70 mM calcein, after which vesicles were formed by five freeze-thaw cycles. Finished LUVs were made by extrusion through two stacked 0.1 μm polycarbonate filters (Nucleopore Filtration Products, Pleasanton, CA) using a Mini-Extruder (Avanti Polar Lipids, Alabaster, AL) with a minimum of 11 passes [52]. The Ames phosphate assay was used to determine the concentrations of phospholipids in the finished products [53].

Calcein leakage experiments were performed in triplicate on a Varian Cary Eclipse fluorimeter with excitation and emission wavelengths of 490 nm and 520 nm, and excitation and emission slit widths of 5 nm. Measurements were carried out in a 1-mL sample volume with mixing and kept at 37 °C using a Peltier temperature control device. Calcein-encapsulated LUVs were diluted in leakage buffer to a final phospholipid concentration of 10 μM. The calcein-loaded LUVs were supplemented by LUVs prepared in calcein-free leakage buffer to increase lipid concentrations for studies of peptide to lipid molar ratios (P/L). Using the kinetics application in the Cary Eclipse software package, the baseline fluorescence was monitored for 1 min (F_o), after which peptide was added to a final concentration of 1 μM. After the addition of peptide the increase in fluorescence due to the release of the calcein dye from the vesicles (F) was monitored for 10 min. In cases where low levels of leakage were observed, further assays at lower peptide to lipid ratios were not pursued. The total calcein fluorescence (F_T) was determined by the addition of Triton X-100 to a final concentration of 0.1%.

3. Results

3.1. Initial peptide design

After analyzing the sequences and three-dimensional structures of the four chemokines, a common Pro residue was chosen as the starting point for the C-terminal α-helix peptides. In all four cases, this residue is at the start of the turn connecting the β-sheet to the carboxy-terminal α-helix. Because of its unique cyclic structure, a Pro residue can also be advantageous as it would protect against exoproteolytic degradation at the N-terminus. The subsequent residues of the chemokines make up the remainder of the peptides, resulting in sequences that are 19–21 residues in length. The peptides were named according to the corresponding residue numbers of the parent chemokines: MIP-3α_{51-70}, IL-8_{53-72}, NAP-2_{50-70}, and TC-1_{50-68}. The resulting IL-8-derived sequence coincides with a fragment recovered after acid hydrolysis [31]. The previously studied 12-residue peptide, MIP-3α_{59-70} [20], was also included for comparison with MIP-3α_{51-70}. Amino acid sequences of the peptides and some sequence-based properties are found in Table 2.

3.2. α-Helical content prediction in aqueous solution

The C-terminal chemokine peptides were analyzed for their α-helical propensity by AGADIR (Table 2) [54,55]. AGADIR is a fast and reliable computational method for predicting the α-helical content of isolated monomeric peptides in aqueous solution, taking into account

Table 2
Sequences and net charges of the C-terminal chemokine peptides.

Peptide	Sequence	Net charge	% helicity[a]
MIP-3α_{51-70}	PKQTWVKYIVRLLSKKVKNM	+6	3.9
MIP-3α_{59-70}	IVRLLSKKVKNM	+4	0.3
IL-8_{53-72}	PKENWVQRVVEKFLKRAENS	+2	1.5
NAP-2_{50-70}	PDAPRIKKIVQKKLAGDESAD	+1	1.3
TC-1_{50-68}	PDAPRIKKIVQKKLAGDES	+2	1.3

[a] As predicted by AGADIR [54,55] based on the amino acid sequence.

the energetic contributions of intrinsic helical propensities, side-chain–sidechain interactions and main-chain to main-chain hydrogen bonds. The algorithm is generally used to evaluate peptide domains that have been isolated from larger proteins [56,57]. Therefore, AGADIR presents a tool for unbiased structure prediction of peptides independent of their conformation in the parent protein. The predicted α-helical contents in the peptides are consistently low with the highest proportion being 3.9% for MIP-3α_{51-70} and the lowest value belonging to the shortest peptide, MIP-3α_{59-70}. Hence, these peptides likely do not retain their native secondary structures in aqueous solution. This is in agreement with AGADIR values calculated for canonical antimicrobial peptides such as magainin-2 (0.4%) that are known to require a membranous or membrane-mimetic environment to fold into α-helices [23,24,58].

3.3. Circular dichroism spectroscopy

Far-UV CD spectra were acquired at room temperature to investigate the secondary structures of the C-terminal peptides (Fig. 1). In aqueous solution (Fig. 1A), the majority of the peptides had no specific backbone conformation, in agreement with the predictions calculated by the AGADIR program. The lack of structure in water for IL-8$_{53-72}$ disagrees with previously reported CD spectroscopy data presented for a very similar peptide that lacked the N-terminal Pro residue that suggested stable α-helical conformation in aqueous buffer [32]. Spectra were also acquired for IL-8$_{53-72}$ under the same experimental conditions used in the earlier study (0.1 mM peptide, 10.0 mM sodium phosphate, pH 5.5) and the expected profile characteristic of random coil structure was once again observed (Supplementary Fig. 1).

CD spectra of these peptides were also acquired in the presence of increasing concentrations of the co-solvent 2,2,2-trifluoroethanol (TFE). TFE/water mixtures are often used to determine the α-helical propensity of peptides. Moreover they are sometimes used for structural studies of antimicrobial peptides as membrane mimetic solvents and they have been found to exert the same structural influence on the peptides as the addition of sodium dodecyl sulfate (SDS) or dodecylphosphocholine (DPC) micelles [59,60]. Trifluoroethanol is also widely used as a cosolvent to induce α-helical structure in other peptides and proteins [61]. As the TFE content increased, the random coil signature for the five chemokine peptides quickly disappeared and an increase in α-helical content was observed with the typical double minima at 208 and 222 nm. Representative scans of the peptides in 40% TFE are shown in Fig. 1B.

The method SELCON3 [39,40] was used for the analysis of the α-helical content of the chemokine peptides (Fig. 1C). The reference set used for curve fitting included 50 proteins, 13 of which were membrane proteins. Because this did not include any peptides, % α-helicity values are approximate. For TFE concentrations increasing from 0% up to 40%, the helicities of the peptides increased until they reach near maximal levels. MIP-3α_{51-70} in particular had a stronger α-helical propensity than the other peptides, as its helicity increased sharply at a lower TFE concentration, and it had considerably higher α-helical content compared to the other peptides. The α-helicities of the other chemokine peptides increased marginally beyond 40% TFE and the α-helicity of the shorter MIP3α_{59-70} displays the most shallow change with increasing TFE concentrations (Fig. 1C).

3.4. NMR structure determination

Due to the lack of regular structure of the C-terminal peptides in aqueous solution, a membrane-mimetic solvent was utilized for detailed structural analysis by NMR spectroscopy. Traditional 2D ^{1}H TOCSY and NOESY NMR spectra were acquired for the C-terminal chemokine peptides at 25 °C dissolved in a mixture of 4:4:1 chloroform:methanol:water. This organic co-solvent system has

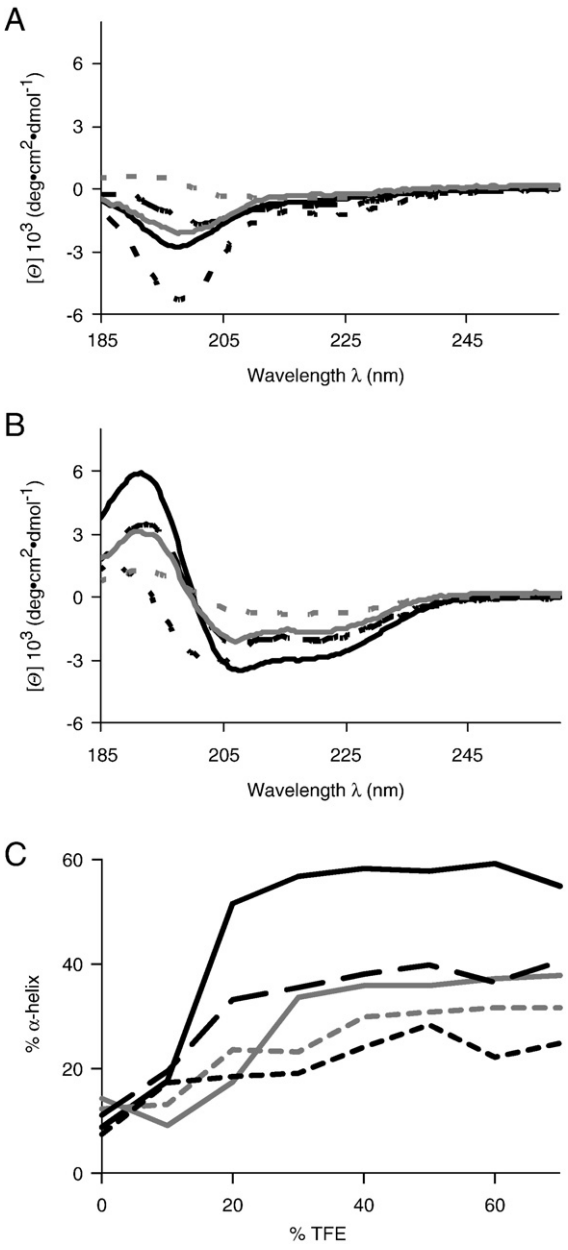

Fig. 1. Far-UV circular dichroism spectra of the C-terminal chemokine peptides in (A) water and (B) 40% TFE. (C) % α-helicity of the peptides at various concentrations of TFE estimated by curve-fitting with the SELCON 3 program [39,40]. The reference set used for curve fitting is based on protein data and therefore % α-helicity values are approximate for the peptides studied here. Spectra were acquired at ambient temperature, and the plots for the peptides (10 μM) are as follows: MIP-3α_{51-70}, solid black; MIP-3α_{59-70}, black short dashes; IL-8$_{53-72}$, long dashes; NAP-2$_{50-70}$, solid gray; TC-1$_{50-68}$, gray short dashes.

previously been used to mimic membrane systems in NMR studies of membrane proteins and peptides [62–64]. The NOESY spectrum of MIP-3α_{51-70} in this co-solvent shows better defined correlations compared to previously acquired spectra of the same peptide bound to SDS micelles (Supplementary Fig. 2) [21]. This is due to the higher effective molecular weight of the micelle/peptide complexes, resulting in broadened signal linewidths. Therefore, the use of the nonpolar solvent mixture, which also has a lower viscosity, improves the quality of the spectra and facilitates the peak assignments and subsequent structure calculations. The NOESY for MIP-3α_{59-70} in 4:4:1 chloroform:methanol:water, however, did not give enough peaks for proper assignments, and therefore its structure was calculated in the membrane-mimetic environment of SDS micelles.

Table 3
Structural statistics for the twenty final NMR structures of the C-terminal chemokine peptides.

	MIP-3α$_{51-70}$	MIP-3α$_{59-70}$	IL-8$_{53-72}$	NAP-2$_{50-70}$	TC-1$_{50-68}$
No. of distance restraints					
Unambiguous NOEs	300	227	247	308	345
Ambiguous NOEs	81	17	66	25	18
Total NOEs	381	244	313	333	363
Broad dihedral restraints	17	10	13	16	14
Global RMSDs					
Backbone (Å)	0.849	0.729	2.128	1.547	1.359
Heavy atom (Å)	1.541	1.386	2.702	2.233	1.927
α-helix RMSDs[a]					
Backbone (Å)	0.407	–	0.436	0.364	0.449
Heavy atom (Å)	1.057	–	1.099	1.123	1.057
α-helix RMSDs vs. full chemokines[b]					
Backbone (Å)	0.61	–	0.65	0.57	0.69
Heavy atom (Å)	1.58	–	1.61	1.69	1.68
Ramachandran (%)[c]					
Most favored	74.7	61.5	79.4	65.6	72.0
Additionally allowed	24.7	37.5	20.6	33.2	27.7
Generously allowed	0.6	1.0	0	1.2	0.3
Disallowed	0	0	0	0	0
α-helix hydrophobic moment (μ_H) [a,d]	3.91	–	4.30	2.43	2.43

[a] α-helix residues are defined as: Thr$_4$–Lys$_{16}$ for MIP-3α$_{51-70}$, Trp$_5$–Leu$_{14}$ for IL-8$_{53-72}$, Pro$_4$–Leu$_{14}$ for NAP-2$_{50-70}$ and TC-1$_{50-68}$.
[b] Structures of the chemokine structures are from PDB as follows: 2HCI, MIP-3α ; 1IKL, IL-8; 1NAP, NAP-2 and TC-1 (a structure of TC-1 is not available).
[c] As determined by Laskowski et al. [47].
[d] Computed using the Totalizer module of MPEx (http://blanco.biomol.uci.edu/mpex).

The failure of the α-helix-promoting organic solvent to induce a stable structure for the 12-mer MIP-3α$_{59-70}$ peptide is probably due to its low α-helical propensity which is evidenced by the CD data (Fig. 1).

Statistics for the twenty final NMR structures of each peptide are listed in Table 3. Hydrophobic moments (μ_H) for the α-helical portions of the 18–20-mer peptides are also reported and can be used as estimates of α-helical amphipathicities. The long C-terminal peptide structures show a well defined α-helix of three to four turns flanked by poorly defined ends. As is commonly observed, RMSDs for the central helical regions, which span between nine to thirteen residues, are considerably lower compared to those of the full length peptides. The helical regions are well defined by medium range NOE distance restraints ($i,i+2$; $i,i+3$; $i,i+4$) that are classically associated with α-helices (data not shown). In the intact chemokines, the sidechains of the hydrophobic residues in the amphipathic α-helices point towards the interior of the proteins while the charged residues are solvent-exposed. The nonpolar solvent provides a similar stabilizing environment for the hydrophobic portion of the helix and it promotes the formation of a helix in the peptide.

MIP-3α$_{51-70}$ has the longest stable α-helix (Fig. 2A), with the Ramachandran plot showing the highest number of φ and ψ backbone dihedral angles in the α-helical region (not shown). Its α-helix spans four turns from Thr4 to Lys16 with a high degree of amphipathicity ($\mu_H = 3.91$). Lys7, Arg11 and Lys15 make up the positively charged side, which also includes the polar Ser14 sidechain. The hydrophobic face consists of Trp5, Val6, Tyr8, Ile9, Val10, Leu12 and Leu13, but a protruding Lys16 is also present. The unstructured ends flanking the α-helix are polar and have two more positively charged residues, Lys2 and Lys18.

In contrast, the short peptide, MIP-3α$_{59-70}$, does not form a stable α-helix in SDS micelles (Fig. 2C). Particularly for the first five amino acid residues, there are only two medium range NOE peaks characteristic of an α-helix conformation. The RMSD for the entire backbone is 0.729 Å with the slightly higher deviations coming from the end N- and C-terminal residues. MIP-3α$_{59-70}$ is also amphipathic, but unlike MIP-3α$_{51-70}$, the division between the hydrophobic and cationic regions is perpendicular to the length of the peptide. The N-terminal side of the peptide is comprised of Ile1, Val2, Leu4 and Leu5, while the C-terminal side includes the charged sidechains of Lys7, Lys8, Lys10 and the polar end residues Gln11 and Met12.

The α-helix of IL-8$_{53-72}$ is in agreement with the available solution structure of intact IL-8 (Fig. 3) [65]. In the ensemble of final peptide structures, the helix is shorter than what has been previously predicted by a homology and energy-based model [32]. The α-helix is again amphipathic and Trp5, Val6, Val9, Val10, Phe13 and Leu14 contribute to the high hydrophobic moment ($\mu_H = 4.30$). The cationic surface composed of Arg8, Lys 12 and Lys15 is somewhat neutralized by the presence of Glu11. Similar to MIP-3α$_{51-70}$, the ends of the peptide are very polar, although they include mixtures of oppositely charged sidechains, specifically Lys2 and Glu3 near the N-terminus and Arg16 and Glu18 at the C-terminal side of the peptide.

The three-turn α-helices of NAP-2$_{50-70}$ and TC-1$_{50-68}$ contain the same residues and are less amphipathic than the other peptides with low hydrophobic moments of 2.43 (Fig. 4). The hydrophobic surface encompasses fewer residues, specifically Ile6, Val10 and Leu14, and these two peptides are devoid of aromatic residues. The positively charged surface is more spread out, involving the Arg5, Lys8, Lys12 and Lys13 sidechains. The presence of Ile9 is mildly disruptive to this cluster of positive charges. The variable ends of these peptides are significant especially because of the two-residue C-terminal extension that distinguishes NAP-2$_{50-70}$ from TC-1$_{50-68}$, which is a critical determinant for the antimicrobial activity in the parent chemokine protein. Two long range distance restraints were observed in the NOESY spectrum of NAP-2$_{50-70}$ between the amide proton of the last residue, Asp21, and the δ and α protons of Lys12. Electrostatic interactions between these residues bring four negatively charged groups, Asp17, Glu18, Asp21 and the carboxyl terminus, from the C-terminal region back over the central α-helix to partly mask the positively charged surface. No correlations were found in the NOESY spectrum for TC-1$_{50-68}$ between any of the C-terminal residues and the central portion of its α-helix.

3.5. Calcein leakage assays

The disruption of a cellular membrane caused by antimicrobial peptides can be assayed by following the fluorescence signal of trapped calcein, a self-quenching dye at high concentrations, as it is released from LUVs [50]. Two different lipid compositions were used to make up the model membrane LUVs: equimolar amounts of zwitterionic ePC and anionic ePG to represent bacterial membranes, and a 2.5:1 ratio of ePC to cholesterol to represent mammalian membranes (Fig. 5) [51].

With both lipid systems, MIP-3α$_{51-70}$ was the strongest leakage-inducing peptide. It caused exceptionally high amounts of intravesicular release from ePC:ePG LUVs with 89.4 ± 1.4% leakage at the low P/L ratio of 1:50 (Fig. 5B). These results point to the bacterial membrane as a major site of action for MIP-3α$_{51-70}$, which has also been demonstrated for other α-helical antimicrobial peptides such as magainin [50] and cecropin [66]. Leakage from ePC:cholesterol LUVs upon the addition of MIP-3α$_{51-70}$ was much lower (26.3 ± 3.5% leakage at a P/L ratio of 1 to 10) compared to ePC:ePG LUVs. This suggests that the peptide would be selective against bacterial membranes over mammalian membranes. In sharp contrast, only very low amounts of leakage were caused by the addition of MIP-3α$_{59-70}$, IL-8$_{53-72}$, NAP-2$_{50-70}$ and TC-1$_{50-68}$ from both LUV types. Even at a high P/L ratio, leakage did not exceed 5% in either model membrane system (Fig. 5B).

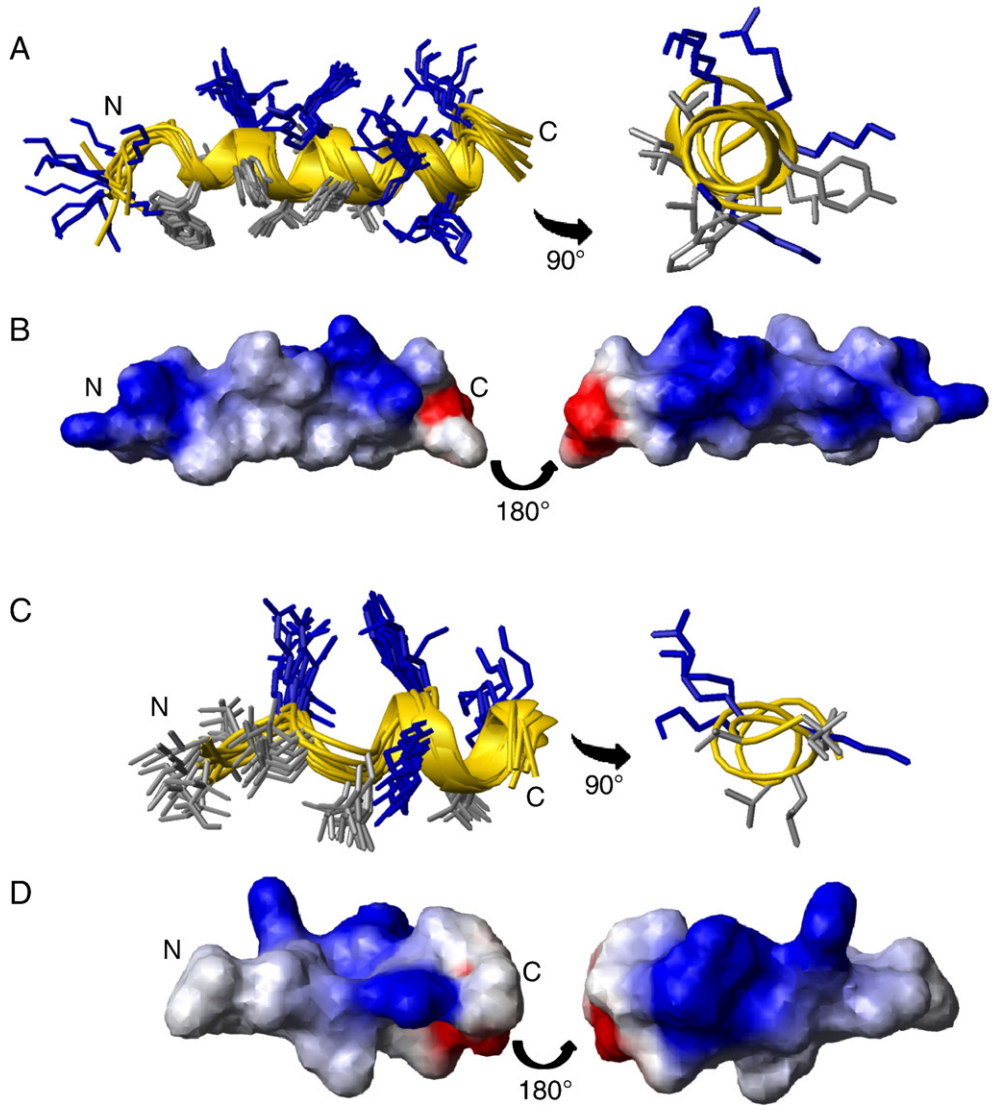

Fig. 2. Solution structures of MIP-3α$_{51-70}$ in 4:4:1 CD_3OH:$CDCl_3$:H_2O (A and B) and MIP-3α$_{59-70}$ in SDS micelles (C and D). (A and C) Ribbon diagram of the ten lowest energy structures, fitted to the backbone atoms of the core α-helix spanning Thr4-Lys16 for MIP-3α$_{51-70}$ (RMSD 0.407 Å) and fitted to the entire backbone for MIP-3α$_{59-70}$ (RMSD 0.729 Å). Hydrophobic sidechains are showcased in gray and positively charged sidechains in blue, with the right panels showing a representative structure with a view perpendicular to the left panels. (B and D) Electrostatic surface plots showing opposite faces of the MIP-3α-derived peptides.

3.6. Biological activities

The chemokine C-terminal peptides were assayed for bactericidal activity using a standard microdilution technique (Table 4) [21,35]. The antimicrobial activities of MIP-3α$_{51-70}$ have been reported previously [20,35]. MIP-3α$_{51-70}$ had high activity against all three tested species, *B. subtilis*, *S. aureus* and *E. coli*. MIP-3α$_{59-70}$, which comprises of only the last 12 residues of the former peptide, was comparatively poor as an antimicrobial and has lost most of the anti-staphylococcal activity. IL-8$_{53-72}$ and NAP-2$_{50-70}$ had moderate and low activity, respectively, against *B. subtilis*. TC-1$_{50-68}$ was not bactericidal against any of the organisms. Hemolytic assays were performed to assess the selectivity of the C-terminal peptides for bacterial over mammalian cells (Fig. 6). MIP-3α$_{51-70}$ was the only peptide with significant hemolytic activity, causing 50% lysis at a concentration of 100 μM.

4. Discussion

Peptide fragments derived from intact proteins do not necessarily preserve their native conformation. This has been most dramatically demonstrated by the spontaneous helix-to-sheet conversion of the antimicrobial bovine lactoferricin peptide when it is released from bovine lactoferrin [67,68]. Such observations reinforce the importance of the overall tertiary structure of proteins where hydrophobic contacts with the remainder of the chemokine proteins stabilizes the fold of the attached C-terminal helix. It also implies that a functional peptide fragment may have altered structure and activity compared to the parent protein [61,67]. Indeed the antimicrobial activity of the bovine peptide lactoferricin far exceeds that of the intact protein [69,70]. The C-terminal chemokine peptides studied here are structurally similar to numerous antimicrobial α-helical peptides. Although the activities of the peptides may match those of the parent proteins as seems to be the case for MIP-3α$_{51-70}$, their mode of action may very well be distinct. This point is further illustrated with MIP-3α$_{59-70}$, which does not seem to be membrane-active like its longer counterpart, but it is somewhat antimicrobial nonetheless.

The C-terminal chemokine peptides studied here were designed with previous studies in mind that highlight the importance of this portion of the proteins to their antimicrobial activity [20,21,31,32,71]. Here, we have experimentally determined the structures which can be compared to computer-generated models for the IL-8 region

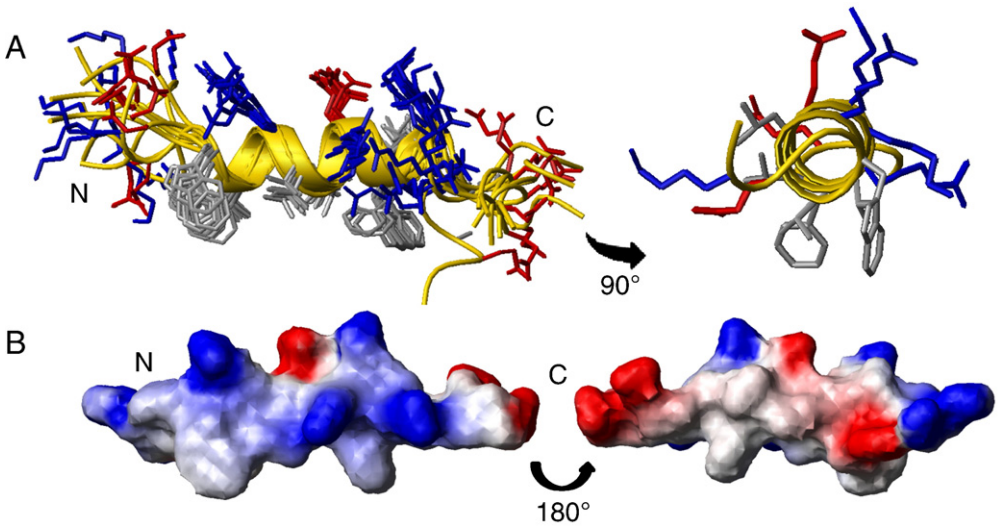

Fig. 3. Solution structure of IL-8_{53-72} in 4:4:1 CD_3OH:$CDCl_3$:H_2O. (A) Ribbon diagram of the ten lowest energy structures, fitted to the backbone atoms of the core α-helix spanning Trp5-Leu14 (RMSD 0.436 Å). Hydrophobic sidechains are showcased in gray, positively charged sidechains in blue, and negatively charged sidechains in red. The right panels show a representative structure with a view perpendicular to the left panels. (B) Electrostatic surface plots showing opposite faces of the peptide.

[31,32]. Such theoretical peptide structures are based on sequence homology comparisons with protein structures. This approach is not ideal because regions of secondary structure elements in proteins do not necessarily fold by themselves in aqueous solution. Rather, their formation depends on stabilizing long range tertiary protein structure interactions or on solvent effects. The CD spectroscopy data presented here clearly indicate that these ~20-mer peptides are unstructured in water and require an environment with some hydrophobicity to form their regular amphipathic secondary structure. This generalization is further supported by the AGADIR calculations, which rely on energy contributions from only short range interactions to predict the α-helical content of a monomeric peptide in aqueous solution [54,55].

Properties of α-helical antimicrobial peptides have been investigated by many groups to aid in the design of successful peptide drug candidates to replace conventional antibiotics. Helical stability and amphipathicity up to optimal degrees promote higher activity [72–74]. However, if the peptide becomes too hydrophobic, the positive charges of a peptide are overshadowed and functional selectivity is lost as the peptide gains cytotoxicity in addition to antimicrobial activity. The high-resolution structures of MIP-3α_{51-70}, IL-8_{53-72}, NAP-2_{50-70}, and TC-1_{50-68} in membrane mimetic solvent show well defined α-helices of differing properties which can be used to compare their activities.

Compared to the other peptides, MIP-3α_{51-70} is the most active peptide. It efficiently induces leakage from vesicles with negatively charged lipid headgroups. This behaviour has been commonly associated with the toroidal pore mechanism of action in which pores are formed in the cytoplasmic membrane that are lined with peptides and interdigitating lipid molecules [75,50], although other mechanisms of membrane permeabilization such as the carpet and sinking raft models cannot be excluded [75,76]. The high activity of MIP-3α_{51-70} also extends to cytotoxicity, with modest levels of leakage observed for the PC/cholesterol vesicles at the low lipid to peptide ratio and significant hemolytic activity. The cytotoxicity is not present in intact MIP-3α where the hydrophobic portion of the α-helix is part of the interior of the chemokine. Thus, there can be potential disadvantages when amphipathic peptide fragments are isolated from intact proteins. Nevertheless, the effective hemolytic concentration of MIP-3α_{51-70} is at least 50-fold greater than the antimicrobial lethal dose concentrations.

Although the shorter MIP-3α_{59-70} peptide is not as potent as MIP-3α_{51-70}, it still has significant activity against *B. subtilis* and *E. coli*. Unlike MIP-3α_{51-70}, MIP-3α_{59-70} does not cause intravesicular leakage from the calcein assays and therefore is not expected to be membrane-active. Its low propensity to form an α-helix in a membranous environment can be attributed to its short length. Furthermore, its sequence starts at Ile59 of MIP3-α and in the native chemokine the α-helix begins at Thr54. The resulting NMR structure of this shorter peptide in SDS micelles shows that its amphipathicity is not aligned along the α-helix axis. Thus, the peptide would not be expected to orient itself parallel to the surface of a bacterial membrane, which has been observed with many α-helical antimicrobial peptides that are associated with the toroidal pore or carpet mechanisms of membrane disruption [77]. The biological activity of MIP-3α_{59-70} is probably due to intracellular interactions following peptide translocation across the membrane [23]. This has generally been found for short peptides as small as six residues [78,79]. Possible inhibition of intracellular functions may stem from some of the peptides' abilities to bind DNA [80,81], although binding to RNA and important proteins cannot be ruled out either.

The positive charges of the IL-8_{53-72} amphipathic α-helix are in part neutralized by the anionic sidechain of Glu11. The entire peptide has a low overall net charge of +2 with additional negatively charged residues at both ends, which are likely responsible for its low membrane-perturbing ability and limited antimicrobial activity. There are discrepancies between the antimicrobial data reported here for IL-8_{53-72} and previous studies of the same peptide. Under our experimental conditions, it was moderately active against *B. subtilis* and inactive against *S. aureus* and *E. coli*. In solid phase inhibition zone area assays, Bjorstad et al. [31] report high growth inhibition of the same peptide against *E. coli* and no activity with *B. subtilis* and *S. aureus* and interestingly, the intact IL-8 chemokine has no anti-*E. coli* activity. In another study, a peptide of the same sequence with the exception of the N-terminal Pro residue was assayed for antimicrobial activity in various media [32]. In solution phase assays, this peptide has no activity against *S. aureus* and *E. coli* in agreement with the data listed here, but high anti-*E. coli* activity was found in blood plasma, serum and whole blood [32]. This difference may be explained by differences in experimental conditions and by the fact that other bacterial strains of the indicated species were used.

As indicated by their low hydrophobic moments, the NAP-2_{50-70} and TC-1_{50-68} α-helices are not greatly amphipathic and are much less hydrophobic than the MIP-3α- and IL-8-derived peptides. However, the C-terminal tail of NAP-2_{50-70} folds back over part of the α-helix, resulting in less solvent-exposed cationicity compared to

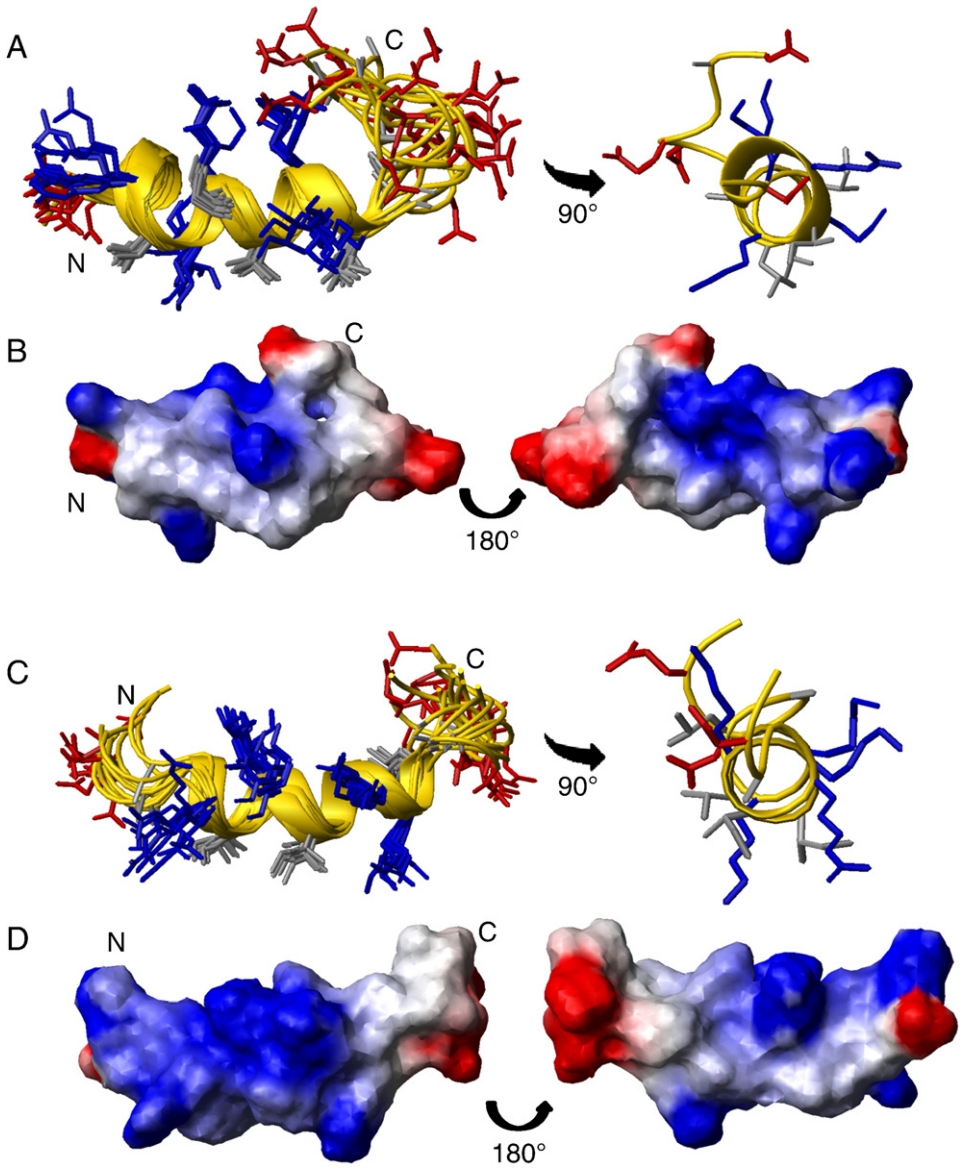

Fig. 4. Solution structures of NAP-2_{50-70} (A and B) and TC-1_{50-68} (C and D) in 4:4:1 CD_3OH:$CDCl_3$:H_2O. (A and C) Ribbon diagram of the ten lowest energy structures, fitted to the backbone atoms of the core α-helices spanning Pro4-Leu14 (RMSD 0.364 Å for NAP-2_{50-70} and 0.449 Å for TC-1_{50-68}). Hydrophobic sidechains are in gray, positively charged sidechains in blue, and negatively charged sidechains in red. The right panels show representative structures with a view perpendicular to the left panels. (B and D) Electrostatic surface plots showing opposite faces of the peptides.

TC-1_{50-68} (Fig. 4). Both peptides were not membrane disruptive as shown by the calcein leakage results and they also lacked antimicrobial activity. The negative charges at the unstructured ends of both peptides may also contribute to this lack of activity, especially in view of the fact that the α-helix itself is very cationic with five Arg/Lys residues. The ends of dermaseptin S9 and lactoferrampin, two recently characterized antimicrobial peptides, have also been shown to play a critical role in their activity [26,82]. The α-helix of the dermaseptin S9 peptide is highly hydrophobic and not amphipathic, but both ends are polar and positively charged. This gives the peptide high antimicrobial potency and low hemolytic activity [82]. Likewise, it was found for lactoferrampin that a relatively uncharged amphipathic helix needed to be followed by a flexible highly positively charged region to make it antimicrobial [25,26]. In the case of NAP-2_{50-70}, the multiple anionic residues on the ends presumably neutralize some of the favorable interactions between the core α-helix and anionic bacterial membranes.

An examination of the overall NAP-2 protein structure helps to understand how its antimicrobial activity may increase when its last two residues are cleaved off to become TC-1 (Fig. 7). The electrostatic potential plot indicates that, although there are positively and negatively charged residues scattered throughout the chemokine surface, the protein is somewhat amphipathic. A strong concentration of cationic charges is observed in the region encompassing the N-terminal region and the C-terminal α-helical domain located in its vicinity, while the remainder of the protein surface is relatively hydrophobic. This positive patch is comprised mostly of residues from the C-terminal α-helix, specifically Arg54, Lys56, Lys57, Lys 60 and Lys61, however Lys17 from the N-terminal portion and Lys41 in the turn between β-strands 2 and 3 also contribute to the positively charged surface region. In the NAP-2_{50-70} and TC-1_{50-68} peptides studied here, Lys17 and Lys41 are not included which may help to explain why they do not exhibit antimicrobial activities. The crystal structure of NAP-2 displays poor electron density for the C-terminal end and as such, only reasonable definition is seen up to Asp66 (Fig. 7) [83]. This flexibility has been observed by an NMR dynamics study as well [84]. The final four residues of NAP-2 include two more anionic residues in addition to the charged carboxy-terminus. This stretch of

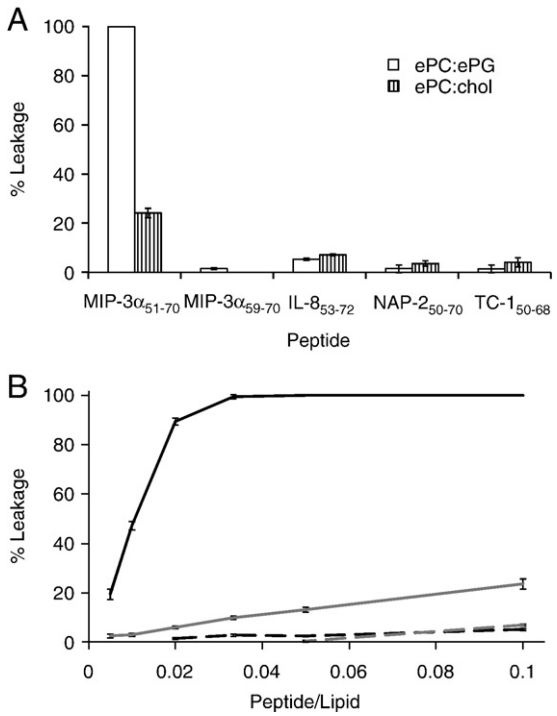

Fig. 5. (A) Calcein leakage caused by the α-helical chemokine peptides from LUVs composed of 1:1 ePC:ePG 2.5:1 ePC:cholesterol at 1:10 peptide:lipid. (B) Calcein leakage profiles of the higher leaking peptides, MIP-3α_{51-70} (black) and IL-8_{53-72} (grey), from ePC:ePG (solid) and ePC:cholesterol (dotted) LUVs at different peptide: lipid ratios. Experiments were performed in triplicate at 37 °C.

highly mobile negatively charged residues may cover the positively-charged patch of NAP-2 and prevent it from being antimicrobial. The removal of Asp71 in TC-1 might stop this region from folding back and could be sufficient to give high antimicrobial potency to the truncated protein.

In conclusion, we have determined the solution structures, membrane perturbation characteristics and antimicrobial activities of a number of carboxy-terminal peptides derived from human chemokines of different microbicidal potencies. We compared three different situations. In the case of MIP-3α, both the protein and the C-terminal helical peptide are known to be active. For IL-8, only the carboxy-terminal peptide shows activity, but not the intact protein. For NAP-2 and TC-1, truncation of the C-terminal end of the protein gives rise to antimicrobial activity. Of all the peptides studied here, MIP-3α_{51-70} shows considerable promise for use as an anti-infective agent given its potent biological activities which are due to the strongly cationic α-helix that forms upon membrane binding. MIP-3α_{59-70}, lacking eight of MIP-3α_{51-70}'s twenty residues, is less antimicrobial and has a structure and mechanism of action that is distinct from its longer counterpart. IL-8_{53-72} folds into an amphipathic α-helix under the same conditions, but the lower overall net charge results in a less potent peptide. Further removal of these negative charges could increase the potency of this IL-8 peptide as we

Table 4
Antimicrobial activities of the C-terminal chemokine peptides.

Peptide	$LD_{99.9}$ (μM)		
	B. subtilis	*S. aureus*	*E. coli*
MIP-3α_{51-70}	≤0.45	1.9	≤0.45
MIP-3α_{59-70}	15	120	30
IL-8_{53-72}	15	>120	>120
NAP-2_{50-70}	120	>120	>120
TC-1_{50-68}	>120	>120	>120

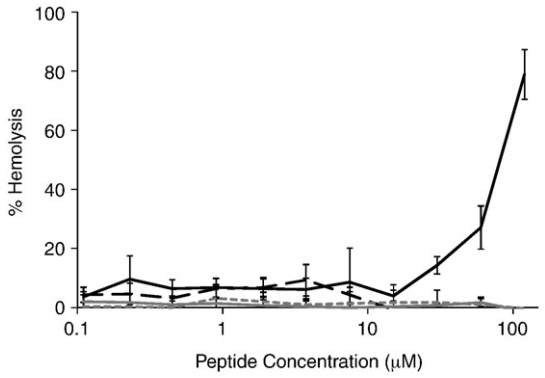

Fig. 6. Hemolytic activities of the α-helical chemokine peptides. Peptide mixtures with human RBCs were incubated for 60 min at 37 °C. The peptides are as follows: MIP-3α_{51-70}, solid black; IL-8_{53-72}, long dashes; NAP-2_{50-70}, solid gray; TC-1_{50-68}, gray short dashes.

have demonstrated for the human lactoferrampin peptide [26]. The α-helices of NAP-2_{50-70} and TC-1_{50-68} as induced by the membrane-mimetic cosolvent are less amphipathic and their anionic ends render

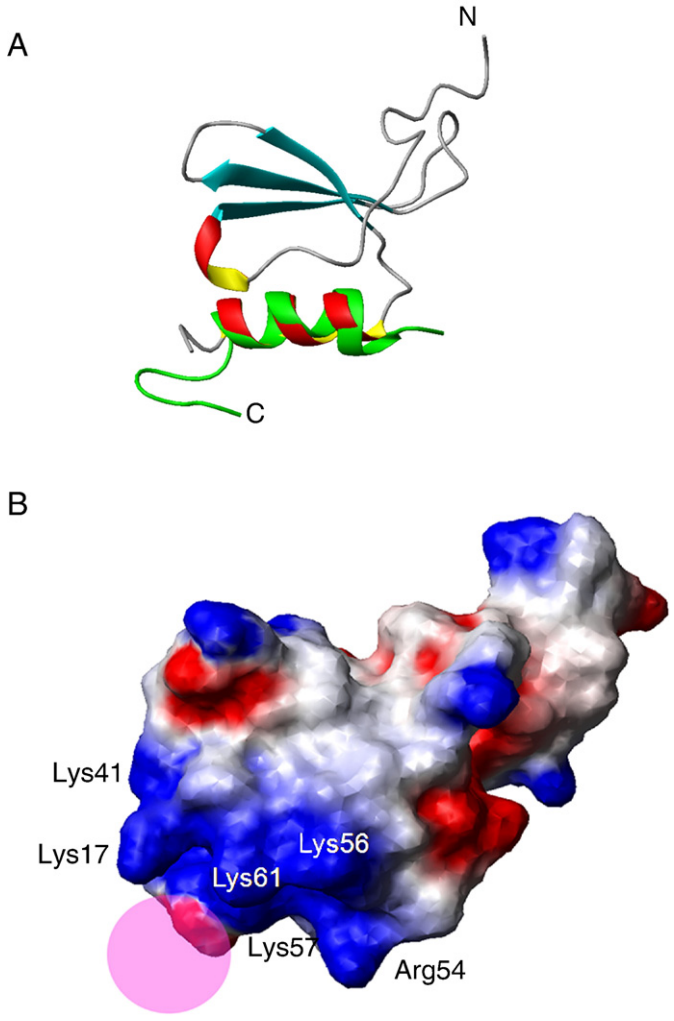

Fig. 7. NAP-2-derived peptides mapped on the NAP-2 crystal structure (PDB 1NAP). (A) Ribbon representation of NAP-2_{50-70} (green) structure solved in membrane mimetic solvent fitted onto NAP-2 through the α-helix. (B) Electrostatic surface plot of NAP-2 with basic residues of the cationic patch highlighted (Lys60 not shown in this view). The last four residues, Glu68–Ser69–Ala70–Asp71, are not included in the crystal structure as they were not identified by the electron density, but they are represented by the pink circle.

the peptides inactive against bacteria, especially for NAP-2_{50-70} where the C-terminal tail was found to fold back to neutralize part of the positively charged portion of its helix.

Acknowledgments

The authors thank Dr. Deane McIntyre for the management and upkeep of the NMR facilities. Operating support for this research was provided by the Institute for Infection and Immunity of the Canadian Institutes of Health Research. L.T.N. is supported by studentship awards from the Alberta Heritage Foundation for Medical Research (AHFMR) and the National Sciences and Engineering Research Council of Canada (NSERC). H.J.V. holds a Scientist Award from the AHFMR.

Appendix A. Supplementary data

Supplementary data associated with this article can be found, in the online version, at doi:10.1016/j.bbamem.2009.11.021.

References

[1] K.L. Brown, R.E. Hancock, Cationic host defense (antimicrobial) peptides, Curr. Opin. Immunol. 18 (2006) 24–30.
[2] M. Dürr, A. Peschel, Chemokines meet defensins: the merging concepts of chemoattractants and antimicrobial peptides in host defense, Infect. Immun. 70 (2002) 6515–6517.
[3] C. Esche, C. Stellato, L.A. Beck, Chemokines: key players in innate and adaptive immunity, J. Invest. Dermatol. 125 (2005) 615–628.
[4] R.E. Hancock, H.G. Sahl, Antimicrobial and host-defense peptides as new anti-infective therapeutic strategies, Nat. Biotechnol. 24 (2006) 1551–1557.
[5] J.E. Meyer, U.H. Beier, T. Gorogh, S. Schreiber, C. Beck, S. Maune, Defensin and chemokine expression patterns in the palatine tonsil: a model of their local interaction, Eur. Arch. Otorhinolaryngol. 263 (2006) 319–326.
[6] A. Pivarcsi, I. Nagy, A. Koreck, K. Kis, A. Kenderessy-Szabo, M. Szell, A. Dobozy, L. Kemeny, Microbial compounds induce the expression of pro-inflammatory cytokines, chemokines, and human beta-defensin-2 in vaginal epithelial cells, Microbes Infect. 7 (2005) 1117–1127.
[7] D.M. Bowdish, D.J. Davidson, R.E. Hancock, Immunomodulatory properties of defensins and cathelicidins, Curr. Top. Microbiol. Immunol. 306 (2006) 27–66.
[8] D. Yang, A. Biragyn, L.W. Kwak, J.J. Oppenheim, Mammalian defensins in immunity: more than just microbicidal, Trends Immunol. 23 (2002) 291–296.
[9] H.M. Linge, M. Collin, P. Nordenfelt, M. Morgelin, M. Malmsten, A. Egesten, Granulocyte chemotactic protein 2 (GCP-2)/CXCL6 possesses membrane disrupting properties and is antibacterial, Antimicrob. Agents Chemother. 52 (2008) 2599–2607.
[10] D. Yang, Q. Chen, D.M. Hoover, P. Staley, K.D. Tucker, J. Lubkowski, J.J. Oppenheim, Many chemokines including CCL20/MIP-3alpha display antimicrobial activity, J. Leukoc. Biol. 74 (2003) 448–455.
[11] N.Y. Yount, K.D. Gank, Y.Q. Xiong, A.S. Bayer, T. Pender, W.H. Welch, M.R. Yeaman, Platelet microbicidal protein 1: structural themes of a multifunctional antimicrobial peptide, Antimicrob. Agents Chemother. 48 (2004) 4395–43404.
[12] K. Lohner, E.J. Prenner, Differential scanning calorimetry and X-ray diffraction studies of the specificity of the interaction of antimicrobial peptides with membrane-mimetic systems, Biochim. Biophys. Acta 1462 (1999) 141–156.
[13] D.M. Hoover, C. Boulègue, D. Yang, J.J. Oppenheim, K. Tucker, W. Lu, J. Lubkowski, The structure of human macrophage inflammatory protein-3α/CCL20, J. Biol. Chem. 277 (2002) 37647–37654.
[14] R.I. Lehrer, T. Ganz, Defensins of vertebrate animals, Curr. Opin. Immunol. 14 (2002) 96–102.
[15] G. Maisetta, M. Di Luca, S. Esin, W. Florio, F.L. Brancatisano, D. Bottai, M. Campa, G. Batoni, Evaluation of the inhibitory effects of human serum components on bactericidal activity of human beta defensin 3, Peptides 29 (2007) 1–6.
[16] M. Pazgier, A. Prahl, D.M. Hoover, J. Lubkowski, Studies of the biological properties of human beta-defensin 1, J. Biol. Chem. 282 (2007) 1819–1829.
[17] D. Yang, O. Chertov, S.N. Bykovskaia, Q. Chen, M.J. Buffo, J. Shogan, M. Anderson, J.M. Schröder, J.M. Wang, O.M. Howard, J.J. Oppenheim, Beta-defensins: linking innate and adaptive immunity through dendritic and T cell CCR6, Science 286 (1999) 525–528.
[18] M. Baba, T. Imai, M. Nishimura, M. Kakizaki, S. Takagi, K. Hieshima, H. Nomiyama, O. Yoshie, Identification of CCR6, the specific receptor for a novel lymphocyte-directed CC chemokine LARC, J. Biol. Chem. 272 (1997) 14893–14898.
[19] E. Schutyser, S. Struyf, J. Van Damme, TheCC , chemokine CCL20 and its receptor CCR6, Cytokine Growth Factor Rev. 14 (2003) 409–426.
[20] L. Hasan, L. Mazzucchelli, M. Liebi, M. Lis, R.E. Hunger, A. Tester, C.M. Overall, M. Wolf, Function of liver activation-regulated chemokine/CC chemokine ligand 20 is differently affected by cathepsin B and cathepsin D processing, J. Immunol. 176 (2006) 6512–6522.
[21] D.I. Chan, H.N. Hunter, B.F. Tack, H.J. Vogel, Human macrophage inflammatory protein-3{alpha}: protein and peptide NMR solution structures, dimerization, dynamics and anti-infective properties, Antimicrob. Agents Chemother. 52 (2008) 883–894.
[22] Z.A. Malik, B.F. Tack, Structure of human MIP-3alpha chemokine, Acta Crystallogr. Sect. F. Struct. Biol. Cyst. Commun. 62 (2006) 631–634.
[23] R.M. Epand, H.J. Vogel, Diversity of antimicrobial peptides and their mechanisms of action, Biochim. Biophys. Acta 1462 (1999) 11–28.
[24] A. Tossi, L. Sandri, A. Giangaspero, Amphipathic, alpha-helical antimicrobial peptides, Biopolym 55 (2000) 4–30.
[25] E.F. Haney, F. Lau, H.J. Vogel, Solution structures and model membrane interactions of lactoferrampin, an antimicrobial peptide derived from bovine lactoferrin, Biochim. Biophys. Acta 1768 (2007) 2355–2364.
[26] E.F. Haney, K. Nazmi, F. Lau, J.G. Bolscher, H.J. Vogel, Novel lactoferrampin antimicrobial peptides derived from human lactoferrin, Biochimie 91 (2008) 141–154.
[27] F. Porcelli, R. Verardi, L. Shi, K.A. Henzler-Wildman, A. Ramamoorthy, G. Veglia, NMR structure of the cathelicidins-derived human antimicrobial peptide LL-37 in dodecylphosphocholine micelles, Biochemistry 47 (2008) 5565–5572.
[28] A. Bhunia, A. Ramamoorthy, S. Bhattacharjya, Helical hairpin structure of a potent antimicrobial peptide MSI-594 in lipopolysaccharide micelles by NMR spectroscopy, Chem. A Eur. J. 15 (2009) 2036–2040.
[29] L.M. Gottler, A. Ramamoorthy, Structure, membrane orientation, mechanism, and function of pexiganan—a highly potent antimicrobial peptide designed from magainin, Biochem. Biophys. Acta 1788 (2009) 1680–1686.
[30] A. Ramamoorthy, Beyond NMR spectra of antimicrobial peptides: dynamical images at atomistic resolution and functional insights, Solid State NMR 35 (2009) 201–207.
[31] A. Bjorstad, H. Fu, A. Karlsson, C. Dahlgren, J. Bylund, Interleukin-8-derived peptide has antibacterial activity, Antimicrob. Agents Chemother. 49 (2005) 3889–3895.
[32] N.Y. Yount, A.J. Waring, K.D. Gank, W.H. Welch, D. Kupferwasser, M.R. Yeaman, Structural correlates of antimicrobial efficacy in IL-8 and related human kinocidins, Biochim. Biophys. Acta 1768 (2007) 598–608.
[33] C. Schumacher, I. Clark-Lewis, M. Baggiolini, B. Moser, High- and low-affinity binding of GROα and neutrophil-activating peptide 2 to interleukin 8 receptors on human neutrophils, Proc. Natl. Acad. Sci. 89 (1992) 10542–10546.
[34] J.E. Ehlert, F. Petersen, M.H. Kubbutat, J. Gerdes, H.D. Flad, E. Brandt, Limited and defined truncation at the C terminus enhances receptor binding and degranulation activity of the neutrophil-activating peptide 2 (NAP-2). Comparison of native and recombinant NAP-2 variants, J. Biol. Chem. 270 (1995) 6338–6344.
[35] J. Krijgsveld, S.A.J. Zaat, J. Meeldijk, P.A. van Veelen, G. Fang, B. Poolman, E. Brandt, J.E. Ehlert, A.J. Kuijpers, G.H.M. Engbers, J. Feijen, J. Dankert, Thrombocidins, microbicidal proteins from human blood platelets, are C-terminal deletion products of CXC chemokines, J. Biol. Chem. 275 (2000) 20374–20381.
[36] J. Dankert, J. Krijgsveld, J. van Der Werff, W. Joldersma, S.A. Zaat, Platelet microbicidal activity is an important defense factor against viridans streptococcal endocarditis, J. Infect. Dis. 184 (2001) 597–605.
[37] J.E. Ehlert, J. Gerdes, H.-D. Flad, E. Brandt, Novel C-terminally truncated isoforms of the CXC chemokine β-thromboglobulin and their impact on neutrophil functions, J. Immunol. 161 (1998) 4975–4982.
[38] S.C. Gill, P.H. von Hippel, Calculation of protein extinction coefficients from amino acid sequence data, Anal. Biochem. 182 (1989) 319–326.
[39] N. Sreerama, R.W. Woody, A self-consistent method for the analysis of protein secondary structure from circular dichroism, Anal. Biochem. 209 (1993) 32–44.
[40] N. Sreerama, R.W. Woody, Estimation of protein secondary structure from circular dichroism spectra: comparison on CONTIN, SELCON, and CDSSTR methods with an expanded reference set, Anal. Biochem. 287 (2000) 252–260.
[41] T.L. Hwang, A.J. Shaka, Water suppression that works—excitation sculpting using arbitrary wave-forms and pulsed-field gradients, J. Magn. Reson. A 112 (1995) 275–279.
[42] F. Delaglio, S. Grzesiek, G. Vuister, G. Zhu, G. Pfeifer, A. Bax, NMRPipe: a multidimensional spectral processing system based on UNIX pipes, J. Biomol. NMR 6 (1995) 277–293.
[43] B.A. Johnson, R.A. Blevins, NMRView—a computer-program for the visualization and analysis of NMR data, J. Biomol. NMR 4 (1994) 603–614.
[44] K. Wüthrich, NMR of proteins and nucleic acids, John Wiley & Sons, New York, 1986.
[45] J.P. Linge, S.I. O'Donoghue, M. Nilges, Automated assignment of ambiguous nuclear Overhauser effects with ARIA, Methods Enzymol. 339 (2001) 71–90.
[46] M. Nilges, S.I. O'Donogue, Ambiguous NOEs and automated NOE assignment, Prog. Nucl. Magn. Reson. Spec. 32 (1998) 107–139.
[47] R.A. Laskowski, M.W. MacArthur, D.S. Moss, J.M. Thornton, Procheck—a program to check the stereochemical quality of protein structures, J. Appl. Crystallogr. 26 (1993) 283–291.
[48] R. Koradi, M. Billeter, K. Wuthrich, MOLMOL: a program for display and analysis of macromolecular structures, J. Mol. Graph. 14 (1996) 51–55.
[49] W.C. Wimley, S.H. White, Experimentally determined hydrophobicity scale for proteins at membrane interfaces, Nat. Struct. Biol. 3 (1996) 842–848.
[50] K. Matsuzaki, O. Murase, N. Fujii, K. Miyajima, An antimicrobial peptide, magainin 2, induced rapid flip-flop of phospholipids coupled with pore formation and peptide translocation, Biochemistry 35 (1996) 11361–11368.
[51] D.J. Schibli, L.T. Nguyen, S.D. Kernaghan, O. Rekdal, H.J. Vogel, Structure–function analysis of tritrpticin analogs: potential relationships between antimicrobial activities, model membrane interactions, and their micelle-bound NMR structures, Biophys. J. 91 (2006) 4413–4426.
[52] F. Olson, C.A. Hunt, F.C. Szoka, W.J. Vail, D. Papahadjopoulos, Preparation of liposomes of defined size distribution by extrusion through polycarbonate membranes, Biochim. Biophys. Acta 557 (1979) 9–23.

[53] B.N. Ames, Assay of inorganic phosphate, total phosphate and phosphatases, Methods Enzymol. 8 (1966) 115–118.
[54] E. Lacroix, A.R. Viguera, L. Serrano, Elucidating the folding problem of alpha-helices: Local motifs, long-range electrostatics, ionic-strength dependence and prediction of NMR parameters, J. Mol. Biol. 284 (1998) 173–191.
[55] V. Munoz, L. Serrano, Elucidating the folding problem of helical peptides using empirical parameters, Nat. Struct. Biol. 1 (1994) 399–409.
[56] H.W. Dirr, T. Little, D.C. Kuhnert, Y. Sayed, A conserved N-capping motif contributes significantly to the stabilization and dynamics of the C-terminal region of class alpha glutathione S-transferases, J. Biol. Chem. 280 (2005) 19480–19487.
[57] M. Stupak, G. Zoldak, A. Musatov, M. Sprinzl, E. Sedlak, Unusual effect of salts on the homodimeric structure of NADH oxidase from *Thermus thermophilus* in acidic pH, Biochim. Biophys. Acta 1764 (2006) 129–137.
[58] M.P. Boland, F. Separovic, Membrane interactions of antimicrobial peptides from Australian tree frogs, Biochim. Biophys. Acta 1758 (2006) 1178–1183.
[59] S. Campagna, N. Saint, G. Molle, A. Aumelas, Structure and mechanism of action of the antimicrobial peptide piscidin, Biochemistry 46 (2007) 1771–1778.
[60] J. Gesell, M. Zasloff, S.J. Opella, Two-dimensional 1H NMR experiments show that the 23-residue magainin antibiotic peptide is an α-helix in dodecylphosphocholine micelles, sodium dodecylsulfate micelles, and trifluoroethanol/water solution, J. Biomol. NMR 9 (1997) 127–135.
[61] M. Buck, Trifluoroethanol and colleagues: cosolvents come of age. Recent studies with peptides and proteins, Q. Rev. Biophys. 31 (1998) 297–355.
[62] M.E. Girvin, K.V. Rastogi, F. Abildgaard, J.L. Markley, R.H. Fillingame, Solution structure of the transmembrane H+-transporting subunit c of the F1F0 ATP synthase, Biochemistry 37 (1998) 8817–8824.
[63] H.N. Hunter, A.R. Demcoe, H. Jenssen, T.J. Gutteberg, H.J. Vogel, Human lactoferricin is partially folded in aqueous solution and is better stabilized in a membrane mimetic solvent, Antimicrob. Agents Chemother. 49 (2005) 3387–3395.
[64] M. Schwaiger, M. Lebendiker, H. Yerushalmi, M. Coles, A. Groger, C. Schwarz, S. Schuldiner, H. Kessler, NMR investigation of the multidrug transporter EmrE, an integral membrane protein, Eur. J. Biochem. 254 (1998) 610–619.
[65] K. Rajarathnam, I. Clark-Lewis, B.D. Sykes, 1H NMR solution structure of an active monomeric interleukin-8, Biochemistry 34 (1995) 12983–12990.
[66] W. Wang, D.K. Smith, K. Moulding, H.M. Chen, The dependence of membrane permeability by the antibacterial peptide cecropin B and its analogs, CB-1 and CB-3, on liposomes of different composition, J. Biol. Chem. 273 (1998) 27438–27448.
[67] P.M. Hwang, N. Zhou, X. Shan, C.H. Arrowsmith, H.J. Vogel, Three-dimensional solution structure of lactoferricin B, an antimicrobial peptide derived from bovine lactoferrin, Biochemistry 37 (1998) 4288–4298.
[68] N. Zhou, D.P. Tieleman, H.J. Vogel, Molecular dynamics simulations of bovine lactoferricin: turning a helix into a sheet, Biometals 17 (2004) 217–223.
[69] J.L. Gifford, H.N. Hunter, H.J. Vogel, Lactoferricin: a lactoferrin-derived peptide with antimicrobial, antiviral, antitumor and immunological properties, Cell. Mol. Life Sci. 62 (2005) 2588–2598.
[70] H. Wakabayashi, M. Takase, M. Tomita, Lactoferricin derived from milk protein lactoferrin, Curr. Pharm. Des. 9 (2003) 1277–1287.
[71] M.R. Yeaman, N.Y. Yount, A.J. Waring, K.D. Gank, D. Kupferwasser, R. Wiese, A.S. Bayer, W.H. Welch, Modular determinants of antimicrobial activity in platelet factor-4 family kinocidins, Biochim. Biophys. Acta 1768 (2007) 609–619.
[72] M.S. Castro, E.M. Cilli, W. Fontes, Combinatorial synthesis and directed evolution applied to the production of alpha-helix forming antimicrobial peptides analogues, Curr. Protein Pept. Sci. 7 (2006) 473–478.
[73] Y. Chen, M.T. Guarnieri, A.I. Vasil, M.L. Vasil, C.T. Mant, R.S. Hodges, Role of peptide hydrophobicity in the mechanism of action of alpha-helical antimicrobial peptides, Antimicrob. Agents Chemother. 51 (2007) 1398–1406.
[74] I. Zelezetsky, A. Tossi, Alpha-helical antimicrobial peptides—using a sequence template to guide structure–activity relationship studies, Biochim. Biophys. Acta 1758 (2006) 1436–1449.
[75] D.I. Chan, E.J. Prenner, H.J. Vogel, Tryptophan- and arginine-rich antimicrobial peptides: structures and mechanism of action, Biochim. Biophys. Acta 1758 (2006) 1184–1202.
[76] A. Pokorny, P.F. Almeida, Kinetics of dye efflux and lipid flip-flop induced by delta-lysin in phosphatidylcholine vesicles and the mechanism of graded release by amphipathic, alpha-helical peptides, Biochemistry 43 (2004) 8846–8857.
[77] M. Respondek, T. Madl, C. Gobl, R. Golser, K. Zangger, Mapping the orientation of helices in micelle-bound peptides by paramagnetic relaxation waves, J. Am. Chem. Soc. 129 (2007) 5228–5234.
[78] H.N. Hunter, W. Jing, D.J. Schibli, T. Trinh, I.Y. Park, S.C. Kim, H.J. Vogel, The interactions of antimicrobial peptides derived from lysozyme with model membrane systems, Biochim. Biophys. Acta 1668 (2005) 175–189.
[79] A.J. Rezansoff, H.N. Hunter, W. Jing, I.Y. Park, S.C. Kim, H.J. Vogel, Interactions of the antimicrobial peptide Ac-FRWWHR-NH(2) with model membrane systems and bacterial cells, J. Pept. Res. 65 (2005) 491–501.
[80] S. Shin, J.K. Kim, J.Y. Lee, K.W. Jung, J.S. Hwang, J. Lee, D.G. Lee, I. Kim, S.Y. Shin, Y. Kim, Design of potent 9-mer antimicrobial peptide analogs of protaetiamycine and investigation of mechanism of antimicrobial action, J. Pept. Sci. 15 (2009) 559–568.
[81] C. Marchand, K. Krajewski, H.F. Lee, S. Antony, A.A. Johnson, R. Amin, P. Roller, M. Kvaratskhelia, Y. Pommier, Covalent binding of the natural antimicrobial peptide indolicidin to DNA abasic sites, Nucleic Acids Res. 34 (2006) 5157–5165.
[82] O. Lequin, A. Ladram, L. Chabbert, F. Bruston, O. Convert, D. Vanhoye, G. Chassaing, P. Nicolas, M. Amiche, Dermaseptin S9, an alpha-helical antimicrobial peptide with a hydrophobic core and cationic termini, Biochemistry 45 (2006) 468–480.
[83] M.G. Malkowski, J.Y. Wu, J.B. Lazar, P.H. Johnson, B.F. Edwards, The crystal structure of recombinant human neutrophil-activating peptide-2 (M6L) at 1.9-A resolution, J. Biol. Chem. 270 (1995) 7077–7087.
[84] H. Young, V. Roongta, D.J. Daly, K.H. Mayo, NMR structure and dynamics of monomeric neutrophil-activating peptide 2, Biochem. J. 338 (1999) 591–598.
[85] Q.-J. Li, M. Yao, W. Wong, V. Parpura, M. Martins-Green, N- and C-terminal peptides of hIL-8/CXCL8 are ligands for hCXCR1 and hCXCR2, FASEB J. 18 (2004) 776–778.